Remote Sensing Monitoring of the Bottom Topography in a Shallow Reservoir and the Spatiotemporal Changes of Submerged Aquatic Vegetation Under Water Depth Fluctuations

Zhaoning Gong, Shuang Liang, Xing Wang, and Ruiliang Pu

***Abstract*—Monitoring the growth and distribution of submerged aquatic vegetation (SAV) is crucial to the protection and restoration of the ecosystem of inland reservoirs. Considering the high sensitivity of SAV to water depth fluctuations in Guanting Reservoir, China, in this study, we realized the reconstruction of bottom topography by combining changing water level with a long time series remote sensing technology and explored the spatiotemporal succession law of SAV by analyzing the effect of water depth on the spatiotemporal distribution of SAV. Results of water depth spatial distribution in Guanting Reservoir were obtained by using water and land boundary lines to construct underwater terrain contours. The accuracy of estimated water depth data from remote sensing images was verified with measured water depth data, and the average relative error of water depth estimation results was about 0.25 m. The experimental results show that (1) the SWIR bands of Landsat images could avoid the interference of aquatic vegetation and realize the separation of land and water; and (2) after separating water area from land, an SWIR1_NIR index was used to effectively map SAV distribution in the reservoir. The results also indicate that the distribution of SAV in the reservoir is suitable for the water depth range of 0−2 m. Water depth fluctuations cause changes in the spatial distribution of suitable water depth. It is the main reason for the change of SAV distribution area in the reservoir during the past 20 years.**

***Index Terms*—Bottom topography, remote sensing, submerged aquatic vegetation (SAV), SWIR1_NIR index, water-level-fluctuation zone.**

I. Introduction

CONTROLLED by water gradient, a water-level-fluctuation zone (WLFZ) has dual properties of land and water. It is a special seasonal wetland ecosystem [1]. Fluctuating redox conditions, dynamic exchanges across the water–soil interface, and vegetation decomposition and revegetation in the WLFZ make it a sensitive area for the biogeochemical cycling of redox-sensitive elements, nutrients, and chemical contaminants [2]–[4]. As a part of the WLFZ, submerged aquatic vegetation (SAV) is important for environmental protection in shallow lakes, such as purifying water and maintaining fishery production [5]. Knowledge about its composition and areal distribution as well as interannual variations is crucial for managing and maintaining the balance of reservoir ecosystems [6].

Remote sensing has been widely used in vegetation monitoring. The data obtained by remote sensors, including aerial images or satellite images, have been widely used to map terrestrial and wetland plant communities [7], [8], benthic habitat in rivers and coastal zones [9]. In contrast, relatively few studies have used remote sensing to investigate macrophytes in rivers, lakes, and other freshwater, especially SAV with high conservation interest [10]. Although optical signals are strongly absorbed by water, a few case studies show that remote sensing is a potentially effective tool for large-scale aquatic vegetation surveys. In studying aquatic vegetation, vegetation-index-based methods have been used to identify and monitor common reed communities [11]–[13]. Oyama *et al*. [14] used Landsat/ ETM+ images by combining of visual cyanobacteria index with floating algae index to monitor the level of cyanobacteria. The spectral reflectance of aquatic vegetation is greatly affected by water, and it shows strong absorption in red, near-infrared (NIR), and short wave infrared spectral regions [15]. Villa *et al*. [16] made a good distinction between terrestrial vegetation and aquatic vegetation by adopting normalized difference aquatic vegetation index (NDAVI) and water-adjusted vegetation index (WAVI). However, for medium resolution images, there are few simple and effective methods to distinguish SAV from aquatic vegetation.

SAV spends most of its life underwater and is particularly sensitive to a water level fluctuation. The water level fluctuation has a significant effect on the growth, reproduction, and distribution of SAV in a shallow reservoir [17]. In an inland shallow water ecosystem, the water level changes frequently.

Manuscript received January 13, 2021; revised March 20, 2021 and May 10, 2021; accepted May 12, 2021. Date of publication May 17, 2021; date of current version June 9, 2021. This work was supported in part by the National Natural Science Foundation of China under Grant 41971381 and in part by the Key Program of Beijing Municipal Bureau of Water under Grant TAHP-2018-ZB-YY-490S. *(Corresponding author: Shuang Liang.)*

Zhaoning Gong, Shuang Liang, and Xing Wang are with the College of Resource Environment and Tourism, Capital Normal University, Beijing 100048, China, and also with the Beijing Key Laboratory of Resource Environment and GIS, Beijing Laboratory of Water Resource Security, Capital Normal University, Beijing 100048, China (e-mail: gongzhn@163.com; liangsh1010@163.com; wxing 0603@163.com).

Ruiliang Pu is with the School of Geosciences, University of South Florida, Tampa, FL 33620, USA (e-mail: rpu@usf.edu).

Digital Object Identifier 10.1109/JSTARS.2021.3080692

It usually manifests in fluctuations of different frequencies and amplitudes. Water level fluctuations can directly change light availability in the water and oxygen availability in the sediment [18], [19] and strongly influence pathways of nutrient cycling [20], [21]. Many efforts have been made to study how the fluctuation of water level affects the growth of aquatic vegetation. However, they are generally outdoor or indoor simulations of water level rise to study its effects on aquatic vegetation [22]–[24]. Although the experimental data are sufficient and reliable, it is labor-intensive, costly, and limited by environmental conditions. To solve this problem, satellite remote sensing has become a powerful and effective tool for mapping SAV and detecting its change in a large area and over a long period [25].

At present, few experiments make use of changes in underwater topography and water level for analyzing the dynamic change of water depth and further study its influence on the growth and distribution of SAV. The spatial distribution of water depth in the reservoir can be quickly obtained by remote sensing observation of underwater topography. Various remote sensing methods have been introduced in the past to determine shallow-water bathymetry or bottom topography. Among them, active remote sensing methods [26]–[28] limit their routine use because of their high cost and poor applicability to high-turbidity water bodies. The passive remote sensing methods, such as optical remote sensing images, use bathymetry and spectral information to establish an empirical model and estimate the spatial distribution of water depth [29], [30]. In addition, some research used radiative transfer inverse modeling (or ln ratios of two bands) to estimate water depth [31], [32]. However, the issue complicating these bathymetric approaches is that they work best with clear water. These methods are usually not applicable in inland waters (either laden with phytoplankton or sediments). Feng *et al*. [33] overcame this difficulty in remote sensing observation of underwater topography in Poyang Lake. They used a rapidly changing water level technique to extract water level boundary and construct its bathymetric line to obtain underwater topography. Their study provides a reference for the underwater topography remote sensing observation of the Guanting reservoir. Previous studies have rarely studied the coupling relationship between SAV and its water depth. During 1999–2018, the water level of the Guanting Reservoir showed a gradual decline and a gradual rise. How the inundation duration and water depth affect the growth of submerged vegetation remains to be explored. Therefore, it is necessary to study the diffusion and reduction of submerged vegetation under the fluctuation of water level.

In this study, our objectives were to:

1) map the interannual spatial distribution of SAV in Guanting Reservoir from 1999 to 2018;
2) to extract water level boundary and reconstruct bottom topography; and
3) to analyze the spatiotemporal changes and driving factors of SAV underwater depth fluctuations.

The experimental results are presented and analyzed and relevant issues are discussed.

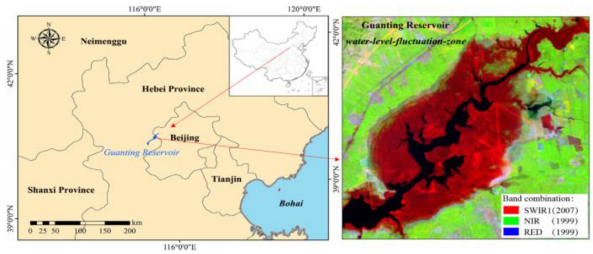

Fig. 1. Overview map of the study area.

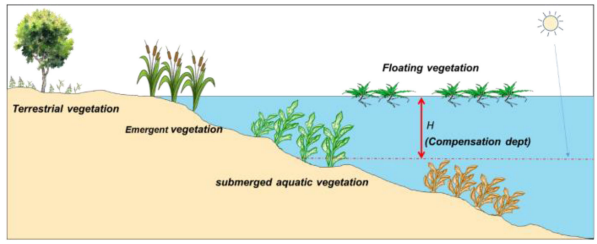

Fig. 2. Schematic diagram of gradient distribution of aquatic vegetation and growth of SAV affected by a light compensation depth.

II. Study Area and Data Preparation

A. Study Area

Guanting Reservoir is one of the drinking water resources, located approximately 100 km northwest of the City of Beijing [34] (see Fig. 1). It plays an important role in flood control, agricultural irrigation, and energy supply for many provinces and cities in China. However, in the late 1980s, the reservoir became severely polluted and the water quality continued to deteriorate until 1990s. In 1997, the reservoir was forced to withdraw from the urban drinking water system. After effective protection and restoration, the water quality of the reservoir improved, and it reopened in 2007 [35]. Due to a long-term interaction of the unique geographical environment, water quality, and climatic conditions, Guanting Reservoir serves as a biodiversity hotspot for an abundancy of wet plants, especially in the upstream reservoir area where the water area is wide and the water depth gradient is obvious.

Landsat images with a large difference in water level were selected and superimposed. As shown in Fig. 1, the region is a WLFZ. Aquatic vegetation distributed in this area is in a gradient space. Different types of wetland plants are zoned, including SAV, floating vegetation, and emergent vegetation (see Fig. 2). SAV is characterized by the fact that most of its bodies are submerged in water, and its survival is significantly affected by the depth of light compensation (see Fig. 2). Typical submerged plants in the reservoir include *Potamogeton pectinatus*, *Myriophyllum spicatum,* and other less common SAV species.

B. Hydrological Data

According to the water situation monitoring report of large- and medium-sized reservoirs published on the official website

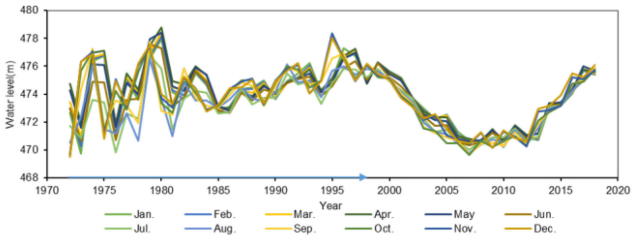

Fig. 3. Water level data of Guanting Reservoir on the 1st day of each month from 1970 to 2018.

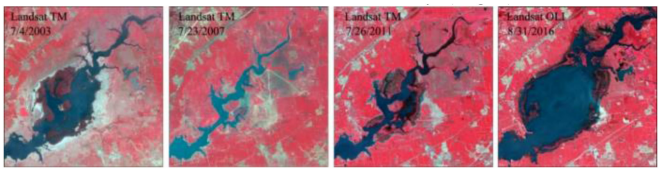

Fig. 4. Landsat images at different periods in the reservoir area. (The false-color composite images were created with RGB vs. NIR, Red, and Green bands).

of Beijing Municipal Water Affairs Bureau, the water level data of Guanting Reservoir from 1970 to 2018 were obtained. Based on the dry–wet alternating rate and the water level variation rate in the subsidence zone of the reservoir, the water level variation from 1970 to 2018 showed divided into three periods (see Fig. 3). The period from 1970 to 1998 was an intermittent fluctuation of water level. From 1999 to 2007, the water level continued to drop and the reservoir area continued to shrink. The water level continued to rise from 2008 to 2018. From 1999 to 2018, the fluctuation of water level in the reservoir completed a full cycle. Periodic fluctuation of water level can be used to better compare the growth and distribution changes of SAV during a fluctuation process. The change of water level in this period has characteristics of periodicity and large amplitude, which are suitable for the research of remote sensing underwater topography reconstruction and the adaptive mechanism of SAV.

C. Satellite Sensors and Dataset

Because of availability, accessibility, and longtime seriality, moderate spatial resolution multispectral satellite imagery, such as Landsat Thematic Mapper (TM), Enhanced TM Plus (ETM+), and Operational Land Imager (OLI), has been used for mapping SAV. In this study, Landsat TM/ETM+/OLI were selected to map the spatial distribution of SAV and extract the water-land boundary (see Fig. 4).

A total of 22 cloud-free images were selected, with 11 used to extract lake boundaries, and 20 used to map SAV (see Table I). Note, some were used to do both. Among them, 20 images were used to extract spatial distribution of SAV, which were selected in July and August of each year to be in the flourishing period of SAV. There were 11 images selected for reservoir boundary extraction, which were mainly obtained through appropriate water level intervals without considering a time limit.

TABLE I
SUMMARY OF THE LANDSAT TM/ETM+/OLI IMAGES USED IN THIS STUDY

Imaging sensor	Acquisition date	Imaging sensor	Acquisition date
Landsat TM	1999/8/2	Landsat TM	2010/8/8
Landsat TM	2000/7/26	Landsat TM	2011/7/26
Landsat TM	2001/7/14*	Landsat ETM+	2012/8/12
Landsat TM	2002/8/9*	Landsat OLI	2013/7/31*
Landsat TM	2003/7/4*	Landsat OLI	2014/8/26*
Landsat TM	2004/7/13	Landsat OLI	2015/7/12*
Landsat TM	2005/7/25	Landsat OLI	2016/8/31*
Landsat TM	2006/7/12	Landsat OLI	2017/3/4*
Landsat TM	2007/8/23*	Landsat OLI	2017/5/23*
Landsat TM	2008/8/2*	Landsat OLI	2017/7/17
Landsat TM	2009/7/20	Landsat OLI	2018/8/21

Note: The images with* were used for extracting reservoir boundary.

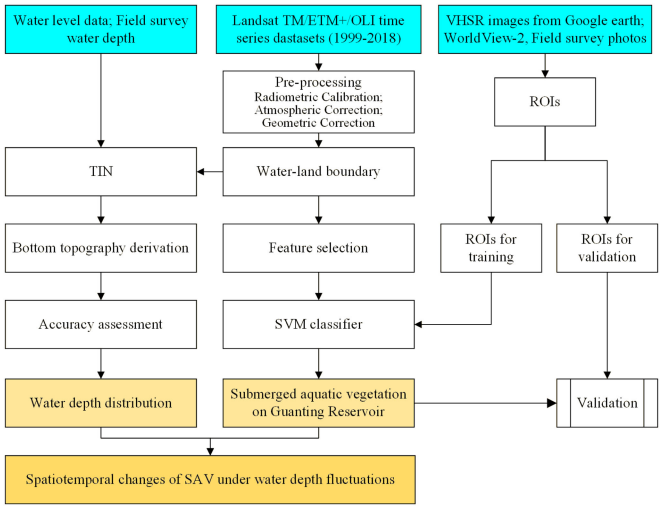

Fig. 5. Workflow of SAV and bathymetry using Landsat images from 1999 to 2018.

III. METHODS

Here we describe our algorithm and workflow to generate annual maps of SAV in Guanting Reservoir from 1999 to 2018 (see Fig. 5). We first extracted the boundary of the submerged area, which includes the water area and the aquatic vegetation area. Second, we identified and mapped the SAV map and the bottom topography map. Third, we analyzed the Spatiotemporal changes of aquatic vegetation underwater level fluctuations

A. Image Preprocessing

Radiometric calibration and atmospheric correction can effectively improve the real spectral radiation value of ground objects [36]. The fast line-of-sight atmospheric analysis of spectral hypercubes module in the ENVI software was applied for atmospheric correction. The existing geometric correction image data in the research area were selected as a reference image and control points were selected for geometric correction.

Since May 31, 2003, the Landsat ETM+ scanning line corrector has lost its function, resulting in overlapping and loss of data on the left and right sides of acquired ground images [37].

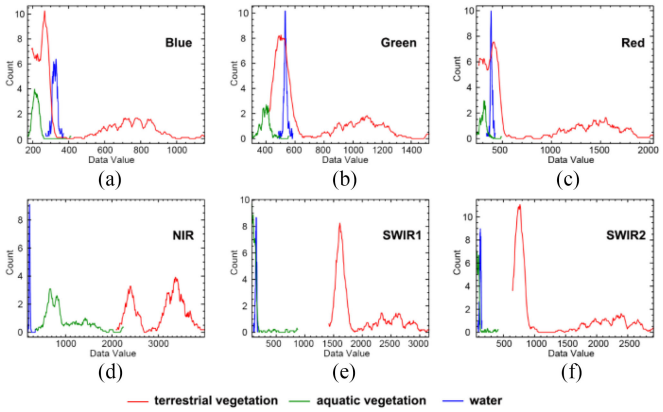

Fig. 6. Histograms of samples of terrestrial vegetation, aquatic vegetation, and water.

In this study, damaged Landsat ETM+ images were repaired using the Landsat gapfill tool of ENVI [38].

B. Water–Land Boundary Delineation

Extracting reservoir boundaries requires separating land and water. Different from the traditional remote sensing extraction methods, the reservoir boundary extracted during vegetation growing season relates to the growth distribution of aquatic vegetation. Therefore, it is very important for us to extract the water–land boundary of the reservoir without the influence of SAV, floating vegetation, and a few emergent vegetation.

The boundary extraction of vegetation seasonal growth in the reservoir should consider the disturbance of aquatic vegetation to the process of boundary identification, rather than simply extracting surface boundary. Landsat data collected in the past 20 years, including three satellite sensors TM, ETM+, and OLI, were selected for the reservoir boundary extraction. One scene of each sensor was randomly selected (i.e., TM acquired on 2003-7-4, ETM+ acquired on 2007-7-23, and OLI acquired on 2016-8-31) for conducting the water and land separation experiment. Samples of terrestrial vegetation, aquatic vegetation, and water were randomly selected in the experiment.

Taking Landsat OLI as an example, samples of terrestrial vegetation, aquatic vegetation, and water were selected, and their histogram distributions of gray values in different bands were calculated. We choose blue, green, red, NIR, short-wave infrared 1 (SWIR1), and short-wave infrared 2 (SWIR2) bands for analysis (see Fig. 6). The coastal band is unique to OLI, but it was not used in this study. It can be seen from Fig. 6 that although the NIR band can distinguish three kinds of features well, a threshold of differentiation between aquatic vegetation and terrestrial vegetation is not clear, and it is easy to be confused. In the SWIR1 and SWIR2 bands, the water and aquatic vegetation are significantly different from the terrestrial vegetation as a whole, and there is a clear distinction between thresholds. The threshold difference between the two types in the SWIR1 (1.55–1.75 μm) band is larger, and the distinction is more significant. The SWIR1 band also significantly separates terrestrial vegetation on TM and ETM+ images. Therefore, the

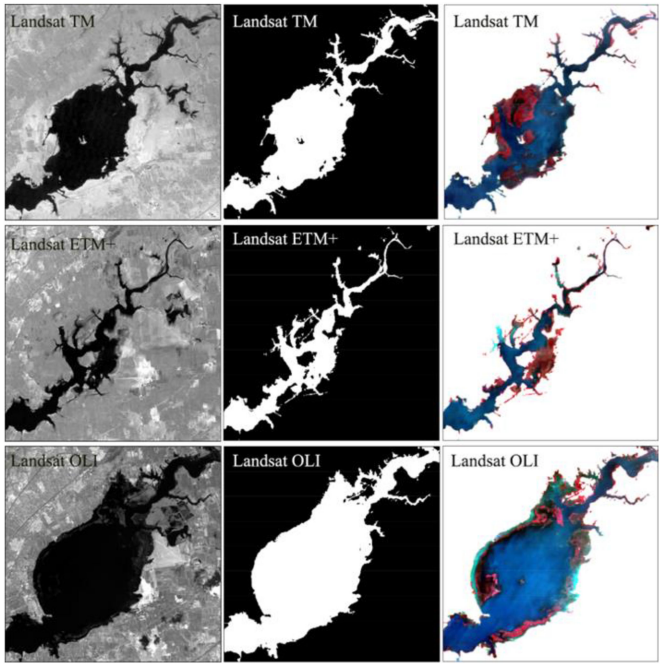

Fig. 7. Extraction of water and land boundaries based on Landsat images in the reservoir. (The first column is SWIR1 single-band display, the second column is the extracted water area, and the third column is the standard false-color composite display in the study area).

SWIR1-band threshold method was chosen to extract the water and land boundary of the reservoir. For each Landsat image, the threshold is determined visually based on the histogram of the SWIR1 band. Finally, the range of dynamic threshold is between 0.06 and 0.12 for different temporal images. A simple SWIR1 band can effectively distinguish aquatic vegetation from terrestrial vegetation, so we did not try to use other water indexes that have little effect. For example, the NDWI [39] indices including the NIR band cannot distinguish between SAV and terrestrial vegetation. Fig. 7 presents the results of land and water boundaries extracted from Landsat images by manual correction and removal of the reservoir water pits outside interference.

C. SAV Remote Sensing Mapping

The aquatic vegetation in Guanting Reservoir mainly includes three life forms: emergent vegetation, floating vegetation, and SAV. In the field surveys conducted in 2016 and 2017, it was found that the floating vegetation was rare and distributed among a small area that was generally smaller than medium resolution pixel size (30 $\times$ 30 m), which was greatly affected by the water background and difficult to identify. Therefore, in this study, two dominant species of aquatic vegetation, emergent vegetation, and SAV, were considered as classification objects without considering floating vegetation.

The stems and leaves of emergent vegetation rise out of the water surface, while those of SAV sink into the water. The reflection spectrum of SAV is more affected by water than that of emergent vegetation, especially in NIR and SWIR bands, in which the incident energy is strongly absorbed by the

TABLE II
VEGETATION INDICES USED IN THE STUDY

Vegetable index	Formula	Source
NDVI	$\frac{\rho_{NIR}-\rho_{RED}}{\rho_{NIR}+\rho_{RED}}$	Rouse *et al.* (1974)
NDAVI	$\frac{\rho_{NIR}-\rho_{BLUE}}{\rho_{NIR}+\rho_{BLUE}}$	[16]
WAVI	$1.5\frac{\rho_{NIR}-\rho_{BLUE}}{\rho_{NIR}+\rho_{BLUE}+0.5}$	[16]
SWIR1_NIR	$\frac{\rho_{SWIR1}-\rho_{NIR}}{\rho_{SWIR1}+\rho_{NIR}}$	Novelli *et al.* (2016)
SWIR2_NIR	$\frac{\rho_{SWIR2}-\rho_{NIR}}{\rho_{SWIR2}+\rho_{NIR}}$	Novelli *et al.* (2016)
GNDVI	$\frac{\rho_{NIR}-\rho_{GREEN}}{\rho_{NIR}+\rho_{GREEN}}$	Gitelson *et al.* (2002)
DVI	$\rho_{NIR}-\rho_{RED}$	Tucker, 1979
EVI	$2.5\frac{\rho_{NIR}-\rho_{RED}}{\rho_{NIR}+6\rho_{RED}-7.5\rho_{BLUE}+1}$	Huete *et al.* (1997)

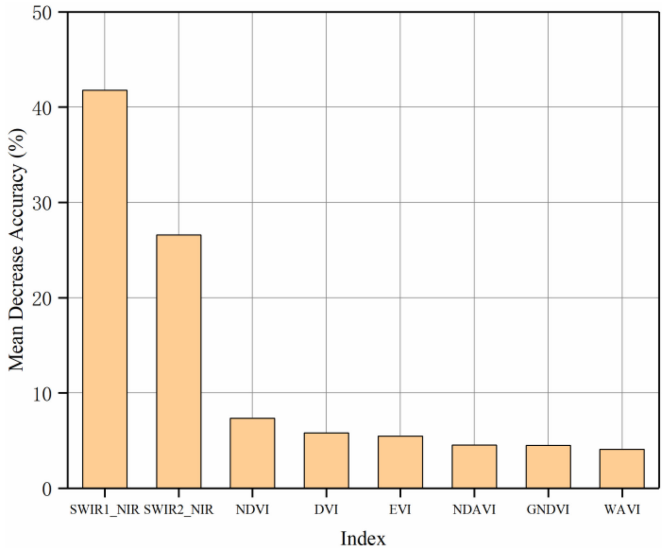

Fig. 8. Evaluation of the importance of random forest characteristic variables.

water. There are obvious differences between SAV and emergent vegetation in these bands. Therefore, according to the spectral characteristics of SAV, this study adopted a fast method to extract the distribution information of SAV from the time series Landsat images at a moderate resolution. According to a submerged state of plants, the type of plants can be judged, namely, the plants above the water surface are emergent vegetation, and the plants below the water surface are SAV.

Based on the results of the previous analysis, we concluded that an effective index for SAV identification should be a combination of SWIR and NIR. In order to find a vegetation index that effectively identifies SAV, we selected eight vegetation indices associated with the two bands (see Table II). A random forest feature selection was used to obtain the importance ranking of different vegetation indices in identifying SAV, and then the best SWIR1_NIR index was found, which could serve as an effective vegetation index for SAV identification (see Fig. 8).

The SWIR1_NIR, SWIR1, SWIR2, and NIR bands can be regarded as sensitive bands for SAV identification and as input features of the support vector machine classifier. For each Landsat image, more than two hundred uniformly distributed pixels are selected as training samples. The SAV maps in Guanting Reservoir were obtained during 1999–2018.

D. Bottom Topography Derivation

The flooded area of Guanting Reservoir has undergone drastic changes during the past 20 years. Except for the perennial flooded area, all other flooded areas' boundaries could be obtained from historical Landsat images. If the water levels of the whole water surface are the same, then in the process of this water level fluctuation, the boundary between land and water can be regarded as the terrain isobathic line [33]. Guanting Reservoir flow velocity is relatively gentle, and thus the water level in the reservoir area is approximately the same.

The underwater topography reconstructed from multiperiod water level data takes into account both the siltation and topography changes which may be caused by years of standing water in the reservoir. Due to the relatively low spatial resolution of the remote sensing data used in the study, boundary lines of water levels extracted from images acquired in corresponding periods located in overlapping areas. Therefore, it is very important to select an appropriate gradient water level boundary for the reconstruction of the subsidence zone. Among the reservoir boundary data extracted from the 22 Landsat images, there were 11 appropriate reservoir water level boundary lines that were selected.

Based on the water level data and corresponding land and water boundaries extracted at the same time, topographic isobaths lines of the reservoir subsidence zone were constructed, and then the topographic reconstruction was carried out by using the isobaths lines. In the topographic reconstruction of this study, the irregular triangular network (TIN) method was constructed by common contour lines [28]. The creation of TIN and the transformation of TIN to the digital surface model (DSM) were all realized by ArcGIS 10.1. To verify the accuracy of underwater topography observation results, the data of measured depth samples were used for comparative purposes.

E. Accuracy Assessment of SAV Mapping and Bottom Topography

The accuracy of the classification results was verified by using high-resolution image. In this study, The WorldView-2 images and very high resolution images from Google Earth acquired in 2013, 2016, and 2017 were used to verify the accuracy of Landsat images derived SAV classification results in their similar periods. For the water boundaries extracted in 2013, 2014, and 2016, we used ArcGIS to generate 500 random points and generate a 30-meter buffer. Each AOI was checked using high-resolution images and labeled the land cover AOIs, and those with vegetation coverage greater than 20% are used. Then a confusion matrix was used to evaluate the classification accuracy.

A field trip for measuring water levels was carried out on July 10, 2017. The elevation of the water level line in the reservoir

TABLE III
SUMMARY FOR THE ACCURACY ASSESSMENT FOR MAPS OF SAV AND NON-SAV IN 2013, 2014, AND 2016 ON GUANTING RESERVOIR

Year	Class	PA	UA	OA
2013	SAV	0.792	0.816	0.844
	Non-SAV	0.879	0.862	
2014	SAV	0.824	0.808	0.852
	Non-SAV	0.870	0.882	
2016	SAV	0.837	0.794	0.861
	Non-SAV	0.873	0.902	

Producer's (PA), user's (UA), and overall (OA) accuracies.

was 475.1 m, and the range of water level change in the WLFZ was 5.42 m. Compared with the maximum water level of 475.79 m (April 4, 2017) used in DSM construction, the water level decreases by 0.69 m. The measured water depth data in the Guanting Reservoir were collected and distributed in different water level gradients. The sample points are distributed as evenly as possible in space. There were a total of 60 measured points, 43 of which were distributed in the WLFZ, and 17 in the inundated area for many years.

IV. RESULTS

A. Accuracy Assessment of the SAV Maps

We carried out the accuracy assessment for maps of SAV in 2013, 2014, and 2016, based on the AOIs for validation (see Table III). The overall classification accuracy was calculated to be 84.4%, 85.2%, and 86.1% in 2013 (July), 2014 (August), and 2016 (August), respectively.

B. Bottom Topography

According to the topographic data of Guanting Reservoir, as long as the maximum water level used in modeling was not exceeded, the spatial distribution of water depth in the inundated area of the reservoir can be judged at any water level. There is no historical record data below the water level elevation value of 469.68 m, and the waters in this region have been inundated for nearly 20 years, so the water depth cannot be directly judged. As of August 21, 2018, the range of water level change in the subsidence zone was at most 6.11 m. In the center of the reservoir, there were some island areas with relatively high topography; the marginal topography presented obvious gradient distribution; and the terrain changes were relatively gentle. In the southern part of the reservoir, the terrain feature was gentle in the north and steep in the south (see Fig. 9).

The data of 43 points in the WLFZ were selected and compared between the measured water depth and the estimated water depth results by the model. It was found that both showed a high consistency, and the determination coefficient of linear fitting was 0.895 (see Fig. 10). The averaged relative error of the water depth results estimated by the model was about 0.25 m. The water depth values of 17 points in the multiyear inundated area were all deeper than 5.42 m.

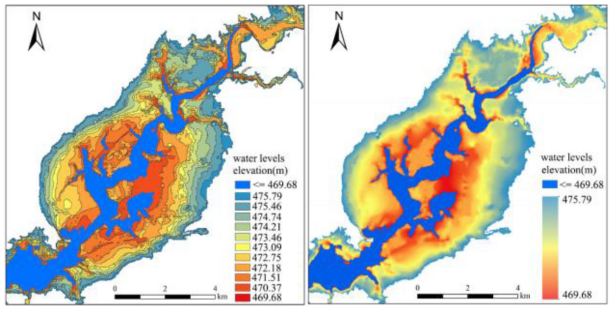

Fig. 9. Spatial distribution of water levels in different time periods in the reservoir.

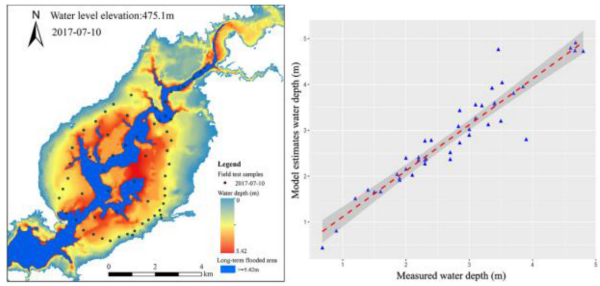

Fig. 10. Water depth and spatial distribution of measured sample points in the reservoir. The measured water depth was compared with the estimated water depth by the model.

C. Spatiotemporal Changes of SAV Under Water Depth Fluctuations

Using long-time series remote sensing data, the spatial distribution information of SAV in Guanting Reservoir during the past 20 years was extracted. Coupled with the topographic data of the WLFZ, the results of the spatial distribution of water depth where SAV was grown during the past 20 years were also obtained (see Fig. 11).

The distribution depth of SAV in the reservoir was all within 3 m, indicating that water depth is one of the important limiting factors affecting SAV spatial distribution (see Fig. 11). SAV in the reservoir was distributed in a zonal pattern paralleling a shoreline, mainly in the southern and northern shorelines. In the central part of the reservoir area, there were SAV communities like "island," which is related to a difference in water depth caused by underwater topography.

V. DISCUSSION

A. Driving Factors for Spatiotemporal Dynamics of SAV in Guanting Reservoir

From 1999 to 2018, the distribution of SAV in reservoir showed a decreasing trend. Since the water reached the trough in 2007 and the water level rose from 2007 to 2018, the inundated area was bare surface for many years, while the SAV from 1999 to 2007 was mostly distributed in the inundated area for many years, such that the SAV area in the reservoir grew slowly from 2007 to 2018 (see Fig. 12). This indicates that the difference

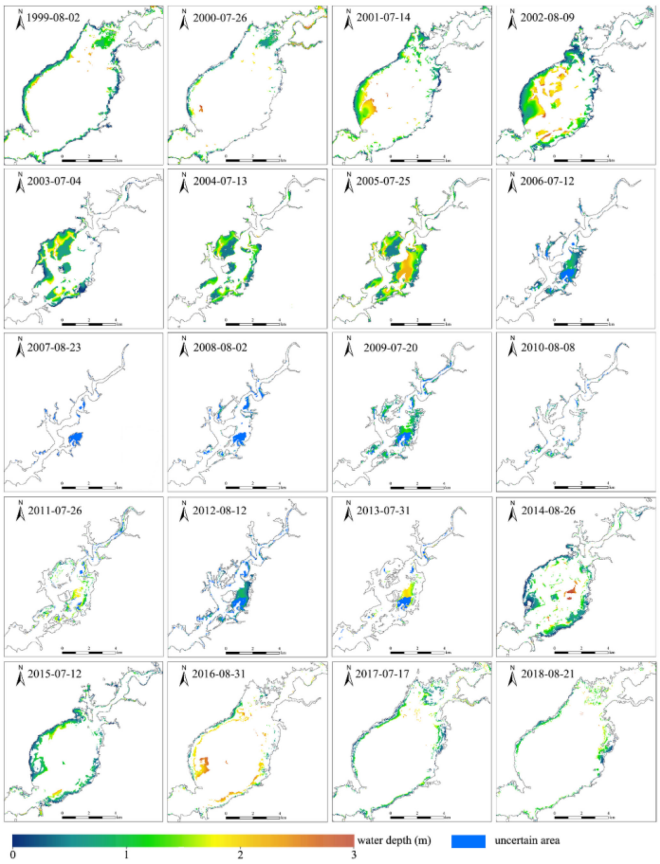

Fig. 11. Spatial distribution of SAV associated with water depth levels from 1999 to 2018.

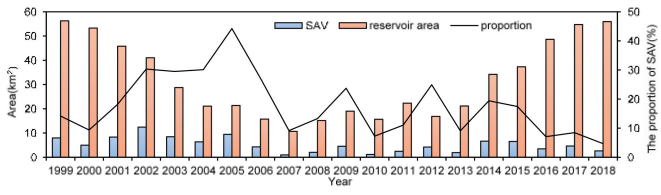

Fig. 12. Changes of water (the reservoir) area and SAV area and the proportion of SAV to the water area from 1999 to 2018.

of surface inundation duration in the reservoir is one of the important limiting factors affecting the formation of its growth distribution pattern. Based on the above analysis of the extracted SAV results, the growth and distribution of SAV in the reservoir area were closely related to the water depth and duration of inundation.

Existing research indicates that the achievement of maximum summer biomass of SAV is affected by both water depth and sediment composition [40]. However, it is difficult for Landsat sensors to judge the sediment type in this study without samples for sediment analysis. Therefore, given the fact that the growth of SAV was affected by the sediment composition, we assumed that its growth distribution was related to the duration of inundation. The duration of inundation affects the sediment composition, which could have been estimated by means of remote sensing.

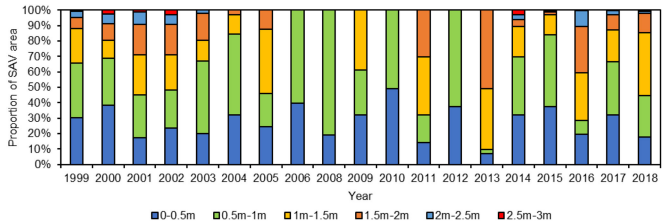

Fig. 13. Proportions of SAV area within different depth gradients to the total SAV area in the reservoir.

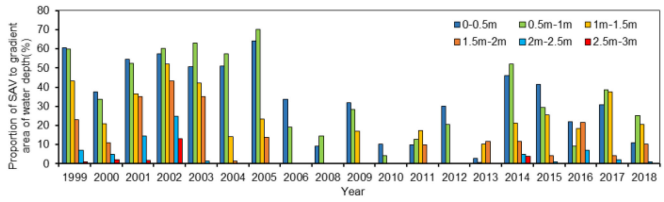

Fig. 14. Proportions of SAV area in different depth gradients to the water area within the water depth range.

This study made statistics on the proportion of SAV in different water depths within 0–3 m and found that the majority of SAV distribution was within 0−2 m, which was an appropriate water depth for SAV to grow in Guanting Reservoir (see Fig. 13). The proportions of SAV distribution with different water depth gradients to the total SAV area within the water depth range were calculated to evaluate their growth and distribution in different water depth gradients (see Fig. 13). In 2007, it was a perennial inundated area with an unknown water depth, so it was not involved in the discussion. It can be found that with the increase in water depth, the proportion of SAV distributed within the water depth range decreased gradually.

The proportions of SAV area in different depth gradients to the water area within the water depth range were calculated as Fig. 14 shown. Under different water depth gradients, the maximum proportion of SAV area was about 60% (see Fig. 14). The distribution area of SAV was relatively high in the appropriate water depth. During the recovery period of water level from 2007 to 2018, the proportion of SAV within different water depth gradients decreased significantly, and the distribution of SAV in the reservoir area was degraded (see Fig. 14).

It is obvious that water depth is an important environmental factor that can affect the growth and distribution of SAV. This is consistent with the findings from other studies [40]–[42]. Bai [43] figured out that water depth was the key ecological factor affecting the root growth of SAV. In this study, the growth and distribution of SAV were significantly affected by the water depth, and the fundamental reason was the influence of optical compensation depth on SAV growth. SAV cannot survive where the optical compensation depth is less than the depth of the water. The fluctuation of water level changed the spatial distribution pattern of water depth in the reservoir. Affected by the fluctuation of water level and attenuation of light, generally, SAV was distributed in waters with a maximum water depth of 12−17m [40]. In fact, the SAV distributes in shallow waters

due to the complex optical properties of water bodies in inland lake reservoirs, including high concentrations of phytoplankton pigments, suspended solids, and CDOM. In Erhai Lake with high water transparency, the maximum water depth of SAV is 6 m, while in Taihu lake with poor water quality, the maximum water depth of SAV is about 2 m only [43]. The water quality of the Guanting Reservoir was slightly better than that of Taihu Lake. Thus, the maximum water depth of SAV in the reservoir was 3 m, of which 2 m was the main distribution area of SAV.

During the period of water level rise from 2007 to 2018, most of the shallow water areas were newly inundated, and the bottom conditions were not suitable for the growth of SAV, which needed to be restored after a period of water inundation. Therefore, the area of SAV in this period was less than that in the same water level in the period from 1999 to 2007 when the water level dropped. With the increase of the water level, the submerged vegetation in the middle of the lake gradually disappeared from 2013 to 2018. Based on the above discussion, it can be found that the growth and distribution of SAV in the reservoir area during the past 20 years were influenced by the water depth and the duration of bottom water inundation.

B. Reliability and Uncertainty of SAV Mapping Using Landsat Data

The series of Landsat TM/ETM+/OLI sensors were selected to conduct this research, and the characteristics of broad-band and moderate spatial resolution were taken into consideration comprehensively. We did not particularly require their high accuracy in identifying SAV, because their accuracy is limited in mapping SAV with weak spectral signals and complex growing environment. The advantage of this data source for our research is its long-time seriality. Therefore, its mapping SAV accuracy could be moderately accurate. If a higher accuracy is required, the data source may need to be changed, which is not consistent with the purpose of this study.

The main factors influencing the performance of classifying SAV could be divided into two groups: intrinsic (i.e., phenological and growth status) and extrinsic (i.e., atmospheric conditions, water quality, and sun-view angle) [44]–[47]. Such a division follows the rationale by Graetz [48], who divided the characteristics of arid rangelands influencing the application of remote sensing into intrinsic and extrinsic factors. For the impact of the water environment, the spectral reflectance of SAV is affected by many factors such as water turbidity/transparency, the distance between the vegetation canopy and the water surface, and the coverage of SAV [49]. Beget *et al*. [50] found that the reflectance in NIR of SAV decreased with the increasing water depth. Therefore, mapping SAV from spectral indices between time periods necessarily involves much uncertainty and error.

Since complex methods considering multiple conditions are difficult to be improved with limited accuracy, this study adopted the simplified idea to carry out research. Such research ignored the complex water environment and atmospheric influence, took the submerged state of vegetation as the discrimination rule, and used strong absorption characteristics of water to effectively map SAV. Our results indicated that rapidly mapping SAV distribution from remote sensing data could achieve a moderate accuracy, which was about 85%. This was a slightly lower accuracy than that of 88% of the SAV mapped by using Zhao's improved decision tree method [47].

A defect of the method developed in this study was that it ignored the situation that the emergent vegetation is submerged. The spectra of submerged emergent vegetation and SAV were similar and affected by the water environment and atmosphere. Few existing studies on mapping submerged plants took this into consideration, but most of the studies were to choose to ignore this point. However, if the water level change is not too large, the SAV mapping errors will not be very high.

C. Limitations of Bottom Topography Derivation

Considering the aquatic vegetation and water body as the submerged area, its boundary line is regarded as the contour line of the surface water level. The bottom topography is generated by interpolation of the water boundary extracted from remote sensing images and water level data. In clear water rivers, optical methods can map bathymetry accurately to depths exceeding 12 m [31], [32]. Compared with radiative transfer inverse modeling, this study did not attempt to estimate water depth from light that penetrates and reflects off of the lake bottom, those avoiding particles in the water column. Therefore, this bottom topography derivation method still works if there is significant material in the water column, such as phytoplankton, cyanobacteria, or sediments.

The lack of sufficient concurrent field water depth data makes absolute validation of the Landsat-based bottom topography impossible. However, it is possible to use indirect evidence to prove the effectiveness of the method. Theoretically, the bottom elevation of most locations is consistent across multiple years, especially in the middle of the lake. Feng *et al*. [33] believe that the uncertainty of the bottom topography is generally 0.5 m, and for most lake areas, the uncertainty may be 0.2 m.

This method has limitations, such as being suitable for lakes with a larger range and slower slope, measured data of water level, less sedimentation or erosion, etc. In addition, the water body information extracted from remote sensing images needs to be accurate to avoid being blocked by vegetation and buildings. In this article, the SWIR1 single-band threshold method is used to avoid the occlusion of the aquatic macrophyte in the Guanting Reservoir. This is also used for the extraction of the water boundary and the establishment of bottom topography in the large lake reservoir with aquatic vegetation.

VI. Conclusion

In this study, by comparing spectral characteristics of different ground objects, a remote sensing method used for effectively mapping SAV was found. Because the light incident energy is strongly absorbed by water, the reflectivity of water and aquatic vegetation in the NIR and SWIR region is low, which forms a relatively obvious contrast with the terrestrial vegetation. The difference between SAV and emergent vegetation was obvious in the combination of NIR with SWIR bands (SWIR1_NIR). By comparing the eight vegetation indexes related to NIR and

SWIR bands, we found that the SWIR1_NIR combination could be used to effectively map SAV distribution, which led to better results.

The spatial distribution of SAV in the reservoir during the past 20 years was obtained, and the results showed that the SAV was zonal in the waters near the shoreline, mainly distributed in the waters on both sides of the south bank and the north bank. In the central part of the reservoir, there would be SAV communities like "islands." The water level in Guanting Reservoir went through a complete fluctuation period from 1999 to 2018, and the distribution area of SAV in Guanting Reservoir generally declined first and then slowly increased.

The water level boundary line and the corresponding water level elevation data extracted by separating water and land from images were used to construct underwater terrain contours in the reservoir area and obtain the spatial distribution of water depths within the reservoir area. Based on the measured bathymetric data for the modeling accuracy verification, it was found that the average relative error of the model bathymetric estimation results was about 0.25 m.

Through the analysis of the coupled effect between SAV and water depth, the spatialtemporal variation characteristics of SAV were explored. It was found that the variation of SAV distribution in the reservoir was greatly affected by the variation of water area within 2 m. The results derived from this study confirmed that the growth of SAV was affected by water depth, but it was also confirmed from the issue of the degradation of SAV at the recovery stage that its growth distribution was also related to the duration of submergence in the water. Since this study did not obtain data of substrate conditions in different periods, this part of the study has not been carried out, which will be considered as the next research plan.

ACKNOWLEDGMENT

The authors would like to the United States Geological Survey (USGS) for providing free Landsat images of Guanting Reservoir. Water levels data are available in the Beijing Water Authority (http://swj.beijing. gov.cn).

REFERENCES

[1] W. Mitsch, J. Lu, X. Yuan, W. He, and L. Zhang, "Optimizing ecosystem services in China," *Science*, vol. 322, no. 5901, 2008, Art. no. 528.

[2] J. Liu *et al.*, "Inorganic sulfur and mercury speciation in the water level fluctuation zone of the three gorges reservoir, China: The role of inorganic reduced sulfur on mercury methylation," *Environ. Pollut.*, vol. 237, pp. 1112–1123, 2018.

[3] F. Wang and J. Zhang, "Mercury contamination in aquatic ecosystems under a changing environment: Implications for the three Gorges reservoir," *Chin. Sci. Bull.*, vol. 58, no. 2, pp. 141–149, 2013.

[4] C. Ye, X. Cheng, W. Liu, and Q. Zhang, "Revegetation impacts soil nitrogen dynamics in the water level fluctuation zone of the three gorges reservoir, China," *Sci. Total Environ.*, vol. 517, pp. 76–85, 2015.

[5] L. Hu *et al.*, "Nutrient removal in wetlands with different macrophyte structures in eastern lake Taihu, China," *Ecol. Eng.*, vol. 36, no. 12, pp. 1725–1732, 2010.

[6] J. Luo *et al.*, "Applying remote sensing techniques to monitoring seasonal and interannual changes of aquatic vegetation in Taihu Lake, China," *Ecol. Indicator*, vol. 60, pp. 503–513, 2016.

[7] M. S. Gilmore *et al.*, "Integrating multi-temporal spectral and structural information to map wetland vegetation in a lower connecticut river tidal marsh," *Remote Sens. Environ.*, vol. 112, no. 11, pp. 4048–4060, 2008.

[8] K. S. Schmidt and A. K. Skidmore, "Spectral discrimination of vegetation types in a coastal wetland," *Remote Sens. Environ.*, vol. 85, no. 1, pp. 92–108, 2003.

[9] E. Vahtmäe, T. Kutser, G. Martin, and J. Kotta, "Feasibility of hyperspectral remote sensing for mapping benthic macroalgal cover in turbid coastal waters—A baltic sea case study," *Remote Sens. Environ.*, vol. 101, no. 3, pp. 342–351, 2006.

[10] P. D. Hunter, D. J. Gilvear, A. N. Tyler, N. J. Willby, and A. Kelly, "Mapping macrophytic vegetation in shallow lakes using the compact airborne spectrographic imager (CASI)," *Aquatic Conservation*, vol. 20, no. 7, pp. 717–727, 2010.

[11] A. Davranche, G. Lefebvre, and B. Poulin, "Wetland monitoring using classification trees and SPOT-5 seasonal time series," *Remote Sens. Environ.*, vol. 114, no. 3, pp. 552–562, 2010.

[12] S. Khanna, M. J. Santos, S. L. Ustin, and P. J. Haverkamp, "An integrated approach to a biophysiologically based classification of floating aquatic macrophytes," *Int. J. Remote Sens.*, vol. 32, no. 4, pp. 1067–1094, 2011.

[13] P. Villa, A. Laini, M. Bresciani, and R. Bolpagni, "A remote sensing approach to monitor the conservation status of lacustrine phragmites Australis beds," *Wetlands Ecol. Manag.*, vol. 21, no. 6, pp. 399–416, 2013.

[14] Y. Oyama, T. Fukushima, B. Matsushita, H. Matsuzaki, K. Kamiya, and H. Kobinata, "Monitoring levels of cyanobacterial blooms using the visual cyanobacteria index (VCI) and floating algae index (FAI)," *Int. J. Appl. Earth Observ.*, vol. 38, pp. 335–348, 2015.

[15] W. Zou, L. Yuan, and L. Zhang, "Analyzing the spectral response of submerged aquatic vegetation in a Eutrophic Lake, Shanghai, China," *Ecol. Eng.*, vol. 57, pp. 65–71, 2013.

[16] P. Villa, A. Mousivand, and M. Bresciani, "Aquatic vegetation indices assessment through radiative transfer modeling and linear mixture simulation," *Int. J. Appl. Earth Observ.*, vol. 30, pp. 113–127, 2014.

[17] R. H. Froend and A. J. Mccomb, "Distribution, productivity and reproductive phenology of emergent macrophytes in relation to water regimes at wetlands of south-western Australia," *Marine Freshwater Res.*, vol. 45, no. 8, pp. 1491–1508, 1994.

[18] M. T. Casanova and M. A. Brock, "How do depth, duration and frequency of flooding influence the establishment of wetland plant communities?," *Plant Ecol.,* vol. 147, no. 2, pp. 237–250, 2000.

[19] E. J. Raulings, K. Morris, M. C. Roache, and P. I. Boon, "The importance of water regimes operating at small spatial scales for the diversity and structure of wetland vegetation," *Freshwater Biol.,* vol. 55, no. 3, pp. 701–715, 2010.

[20] H. Coops and S. H. Hosper, "Water-level management as a tool for the restoration of shallow lakes in the Netherlands," *Lake Reservoir Manage. J.*, vol. 18, no. 4, pp. 293–298, 2002.

[21] G. Pinay, J. C. Clément, and R. J. Naiman, "Basic principles and ecological consequences of changing water regimes on nitrogen cycling in fluvial systems," *Environ. Manage.*, vol. 30, no. 4, pp. 481–491, 2002.

[22] B. M. Deegan, S. D. White, and G. G. Ganf, "The influence of water level fluctuations on the growth of four emergent macrophyte species," *Aquatic Botany*, vol. 86, no. 4, pp. 309–315, 2007.

[23] S. M. Thomaz *et al.*, "Effect of reservoir drawdown on biomass of three species of aquatic macrophytes in a large sub-tropical reservoir (Itaipu, Brazil)," *Hydrobiologia*, vol. 570, no. 1, pp. 53–59, 2006.

[24] V. Vretare, S. E. B. Weisner, J. A. Strand, and W. Granéli, "Phenotypic plasticity in phragmites australis as a functional response to water depth," *Aquatic Botany*, vol. 69, no. 2/4, pp. 127–145. 2001.

[25] Y. Zhang *et al.*, "Global loss of aquatic vegetation in lakes," *Earth-Sci. Rev.*, vol. 173, pp. 259–265, 2017.

[26] B. M. Costa, T. A. Battista, and S. J. Pittman, "Comparative evaluation of airborne LiDAR and ship-based multibeam SoNAR bathymetry and intensity for mapping coral reef ecosystems," *Remote Sens. Environ.*, vol. 113, no. 5, pp. 1082–1100, 2009.

[27] D. Gesch and R. Wilson, "Development of a seamless multisource topographic/bathymetric elevation model of Tampa Bay," *Marine Technol. Soc. J.*, vol. 35, no. 4, pp. 58–64, 2001.

[28] C. Wang and W. D. Philpot, "Using airborne bathymetric lidar to detect bottom type variation in shallow waters," *Remote Sens. Environ.*, vol. 106, no. 1, pp. 123–135, 2007.

[29] P. E. Carbonneau, S. N. Lane, and N. Bergeron, "Feature based image processing methods applied to bathymetric measurements from airborne remote sensing in fluvial environments," *Earth Surf. Processes Landforms*, vol. 31, no. 11, pp. 1413–1423. 2006.

[30] J. C. Sandidge and R. J. Holyer, "Coastal bathymetry from hyperspectral observations of water radiance," *Remote Sens. Environ.*, vol. 65, no. 3, pp. 341–352, 1998.

[31] C. J. Legleiter, D. A. Roberts, W. A. Marcus, and M. A. Fonstad, "Passive optical remote sensing of river channel morphology and in-stream habitat: Physical basis and feasibility," *Remote Sens. Environ.*, vol. 93, no. 4, pp. 493–510, 2004.
[32] C. J. Legleiter and D. A. Roberts, "A forward image model for passive optical remote sensing of river bathymetry," *Remote Sens. Environ.*, vol. 113, no. 5, pp. 1025–1045, 2009.
[33] L. Feng, C. Hu, X. Chen, R. Li, L. Tian, and B. Murch, "MODIS observations of the bottom topography and its inter-annual variability of poyang lake," *Remote Sens. Environ.*, vol. 115, no. 10, pp. 2729–2741, 2011.
[34] W. Luo *et al.*, "Landscape ecology of the guanting reservoir, Beijing, China: Multivariate and geostatistical analyses of metals in soils," *Environ. Pollut.*, vol. 146, no. 2, pp. 567–576. 2007.
[35] X. Wang, Z. Gong, and R. Pu, "Estimation of chlorophyll a content in inland turbidity waters using WorldView-2 imagery: a case study of the Guanting Reservoir, Beijing, China," *Environ. Monit. Assess.*, vol. 190, no. 620, pp. 1–16, Sep. 2018.
[36] G. Chander, B. L. Markham, and D. L. Helder, "Summary of current radiometric calibration coefficients for landsat MSS, TM, ETM+, and EO-1 ALI sensors," *Remote Sens. Environ.*, vol. 113, no. 5, pp. 893–903, 2009.
[37] M. J. Pringle, M. Schmidt, and J. S. Muir, "Geostatistical interpolation of SLC-off landsat ETM+ images," *ISPRS J. Photogramm.*, vol. 64, no. 6, pp. 654–664, 2009.
[38] R. L. Miller, C. Liu, C. J. Buonassissi, and A. Wu, "A multi-sensor approach to examining the distribution of total suspended matter (TSM) in the albemarle-pamlico estuarine system, NC, USA," *Remote Sens.-Basel*, vol. 3, no. 5, pp. 962–974, May. 2011.
[39] S. K. Mcfeeters, "The use of the normalized difference water index (NDWI) in the delineation of open water features," *Int. J. Remote Sens.*, vol. 17, no. 7, pp. 1425–1432, 1996.
[40] P. A. Chambers and J. Kaiff, "Depth distribution and biomass of submersed aquatic macrophyte communities in relation to Secchi depth," *Can. J. Fish. Aquatic Sci.*, vol. 42, no. 4, pp. 701–709, Apr. 1985.
[41] J. A. Strand and S. E. B. Weisner, "Morphological plastic responses to water depth and wave exposure in an aquatic plant (*Myriophyllum spicatum*)," *J. Ecol.*, vol. 89, no. 2, pp. 166–175, 2001.
[42] J. M. Milne, K. J. Murphy, and S. M. Thomaz, "Morphological variation in Eichhornia azurea (Kunth) and Eichhornia crassipes (Mart.) solms in relation to aquatic vegetation type and the environment in the floodplain of the Rio Paraná, Brazil," *Hydrobiologia*, vol. 570, no. 1, pp. 19–25, 2006.
[43] X. Bai, K. Chen, H. Zhao, and X. Chen, "Impact of water depth and sediment type on root morphology of the submerged plant vallisneria natans," *J. Freshwater Ecol.*, vol. 30, no. 1, pp. 75–84, 2015.
[44] S. A. C. Nelson, K. S. Cheruvelil, and P. A. Soranno, "Satellite remote sensing of freshwater macrophytes and the influence of water clarity," *Aquatic Botany*, vol. 85, no. 4, pp. 289–298, 2006.
[45] T. S. F. Silva *et al.*, "Remote sensing of aquatic vegetation: Theory and applications," *Environ. Monit. Assessment*, vol. 140, no. 1, pp. 131–145, 2008.
[46] B. Tan, "Rapid updating of rice map for local government using SAR data and GIS in Zengcheng county, Guangdong province, China," *Remote Sens. Land Res.*, vol. 12, no. 1, pp. 24–27, 2000.
[47] D. Zhao, H. Jiang, T. Yang, Y. Cai, D. Xu, and S. An, "Remote sensing of aquatic vegetation distribution in Taihu lake using an improved classification tree with modified thresholds," *J. Environ. Manage.*, vol. 95, no. 1, pp. 98–107, 2012.
[48] R. D. Graetz, "Satellite remote sensing of australian rangelands," *Remote Sens. Environ.*, vol. 23, no. 2, pp. 313–331, 1987.
[49] Q. Chen *et al.*, "A new method for mapping aquatic vegetation especially underwater vegetation in Lake Ulansuhai using GF-1 satellite data," *Remote Sens.*, vol. 10, no. 8, Aug. 2018, Art. no. 1279.
[50] M. E. Beget and C. M. Di Bella, "Flooding: The effect of water depth on the spectral response of grass canopies," *J. Hydrol.*, vol. 335, no. 3/4, pp. 285–294. 2007.

Zhaoning Gong received the Ph.D. degree in ecohydrology from the Northeast Institute of Geography and Agroecology, Chinese Academy of Sciences, Beijing, China, in 2006.

She is currently a Professor with the College of Resource Environment and Tourism, Capital Normal University, Beijing, China. Her current research interests include GIS and remote sensing and biophysical and biochemical parameters extraction

Shuang Liang was born in Jiangsu, China, in October 1997. He received the B.S. degree in geographic information science from Nanjing Forestry University, Nanjing, China, in 2019. He is currently working toward the M.S. degree in cartography and geographic information system from Capital Normal University, Beijing, China.

His research interests include remote sensing application in ecohydrology.

Xing Wang received M.S. degree in cartography and geographic information system from Capital Normal University, Beijing, China, in 2019.

His research interests include remote sensing landcover classification and ecological remote sensing.

Ruiliang Pu received the Ph.D. degree in cartography and geographic information system from Chinese Academy of Sciences, Beijing, China, in 2000.

He is currently a Professor with the School of Geosciences, University of South Florida, Tampa, FL, USA. His research interests include mapping and characterizing seagrass habitats using spacecraft observations, urban environmental studies, and urban tree canopy mapping/species identification using thermal and high-resolution satellite imagery.